IEEE Access
Multidisciplinary ⋮ Rapid Review ⋮ Open Access Journal

Received March 15, 2021, accepted March 22, 2021, date of publication April 6, 2021, date of current version April 19, 2021.

Digital Object Identifier 10.1109/ACCESS.2021.3071322

Adaptive Neural Command Filtered Control for Pneumatic Active Suspension With Prescribed Performance and Input Saturation

CONG MINH HO[1], DUC THIEN TRAN[2], CONG HUNG NGUYEN[1], AND KYOUNG KWAN AHN[3], (Senior Member, IEEE)

[1]Graduate School of Mechanical and Automotive Engineering, University of Ulsan, Ulsan 44610, South Korea
[2]Department of Automatic Control, Ho Chi Minh City University of Technology and Education, Ho Chi Minh City 70000, Vietnam
[3]School of Mechanical and Automotive Engineering, University of Ulsan, Ulsan 44610, South Korea

Corresponding author: Kyoung Kwan Ahn (kkahn@ulsan.ac.kr)

This work was supported by the Basic Science Program through the National Research Foundation of Korea (NRF) funded by the Ministry of Science and ICT, South Korea under Grant NRF-2020R1A2B5B03001480.

ABSTRACT In this paper, an adaptive neural command filtered backstepping scheme is proposed for the pneumatic active suspension with the vertical displacement constraint of sprung mass and actuator saturation. A quarter car model with a pneumatic spring is first fabricated on the basis of thermodynamic theory to describe the dynamic characteristics. To overcome the lumped unknown nonlinearities and enhance the requirement of modeling precision, the radial basis function neural networks (RBFNNs) are proposed to approximate unknown continuous functions caused by the uncertain body mass and other factors of pneumatic spring. To solve the explosion of complexity problem in the traditional backstepping designs, a proposed command filter control is applied by using the Levant differentiators which approach the derivative of the virtual control signals. Nussbaum gain technique is then incorporated into the controller to avoid the problem of the completely unknown control gain and control directions of a pneumatic actuator. In addition, the prescribed performance function (PPF) is suggested to guarantee that the tracking error of the sprung mass displacement does not violate the constraint boundaries. Based on the command filtered backstepping control with PPF, the Lyapunov theorem is then applied to indicate the system stability analysis. Finally, the comparative simulation examples for the pneumatic suspension are given to verify the effectiveness and reliability of the proposed control.

INDEX TERMS Active suspension systems (ASSs), neural networks (NNs), command filtered control (CFC), input saturation, prescribed performance function.

I. INTRODUCTION

The pneumatic suspension has been widely used in the automotive industry to improve passenger comfort and vehicle handling stability [1], [2]. Compared with the various actuators such as hydraulic [3] or electromagnetic [4], pneumatic actuators are low cost, clean, and high power-to-weight ratio characteristics [5], [6]. Pneumatic springs can provide flexible stiffness and generate the control forces according to various uncertain masses of passengers by controlling the internal pressure [7]. However, the high nonlinearity is one of the drawbacks of pneumatic systems, which will make it difficult and complicated to design the suspension model and control scheme [8]. Besides, it not easy to maintain chassis stability under various loads of passengers due to the presence of unknown parameters in the pneumatic servo system [9].

To overcome the above limitations, many control strategies have been widely used to improve vehicle performance such as optimal control [10], [11], sliding mode control [2], [12], and model predictive control [13], [14]. Although these controllers can improve the suspension performance, they may be sensitive to external disturbances because of the fixed control parameters. To solve the problem of height tracking of pneumatic suspension, the backstepping control was proposed and addressed the parametric uncertainties and unmodeled dynamics [9]. However, a common

The associate editor coordinating the review of this manuscript and approving it for publication was Juntao Fei.

disadvantage in the traditional backstepping design process is the explosion of complexity caused by its virtual controller derivatives, which increases computational complexity [15], [16]. Recently, a dynamic surface control (DSC) method has been developed to address this problem by including a first-order filter in each control design step to approximate these derivatives [17], [18]. But the DSC technique does not consider the errors arising from the first-order filters, which can reduce system control efficiency [19]. To solve the same inherent problem of traditional backstepping design, Farrell *et al.* [20] proposed a command filtered control technique. By using a command filter to approximate the differential coefficient of the virtual control signal at every step of the control design, CFC can obtain better system tracking performance [21]–[23]. Furthermore, the compensating signals are proposed to reject the errors caused by the command filters which can solve the limitation of the dynamics surface approach [24], [25].

Generally, it is well known that the function approximation based intelligent design technique has been shown to be a powerful method for dealing with unknown nonlinearities and uncertainties [26], [27]. In particular, neural networks can provide an effective tool to approximate the unknown functions or parametric uncertainties in the pneumatic systems [28], [29]. Bao *et al.* [30] designed a fuzzy adaptive sliding mode control to enhance passenger comfort and vehicle controllability of the pneumatic active suspension. However, the authors did not consider the robust control system in the presence of unmodeled dynamics, and the transient tracking performance cannot be quantitatively guaranteed in previous designs [31]. Although the neural networks can provide a good approximation ability for unknown continuous functions, the traditional backstepping requires that the repeated differentiation of virtual input must be resolved at each step of the design process [32]. Consequently, the drawback of complexity explosion cannot be handled, and this also limits the applications of traditional backstepping. In this paper, adaptive neural networks-based command filtered backstepping technique has been proposed to improve the performance of the pneumatic active suspension.

Significantly, most of the ASSs did not consider the input saturation problem during the control design process; however, the control performance of pneumatic active suspension can be seriously restricted. In order to improve the control efficiency, the effect of actuator saturation needs to be properly regarded in the control design procedure [33]. Although the input saturation of nonlinear systems can be addressed with an adaptive NNs controller [34], it will be more difficult when control gains are unknown time-varying nonlinearities because of the singularity problems [35]. Besides, the control directions are very important in nonlinear system design because they are not easily detected from the prior knowledge of the signs of the parameters, which makes the control design more complicated and challenging. The previous controllers of ASSs are not designed to accommodate unknown control directions for pneumatic systems. As we have known, the Nussbaum gain technique has been incorporated in the controller to handle the problem of unspecified control coefficient [36], [37]. The main point of Nussbaum's approach is that using the switching functions which can obtain the signs of the control directions [38], [39]. This is suitable to overcome the disadvantage of pneumatic active suspension which involves unknown nonlinear functions and depends on many physical parameters.

Recently, a new control scheme with output constraints called prescribed performance control (PPC) was introduced by Bechlioulis to guarantee the convergence of system outputs, maximum overshoot, and steady-state error into an arbitrarily small predefined region [40]. PPC has been used in many control engineering applications requiring output constraints [41], [42]. Zhang *et al.* [43] proposed a novel proportional-integral approximation-free control by using PPFs for nonlinear robotic systems without employing any function approximation. To stabilize the vertical and pitch displacements of active suspensions with parametric uncertainties, an adaptive control with PPF constraints was proposed by Jing Na in [44]. Liu *et al.* [45] designed an adaptive control scheme to ensure the convergence of the tracking error and maximum overshoot of the suspension system with the PPF constraints and actuator failure. However, these results assume that all the system states are available or directly measurable which is rarely satisfied in practical applications [46], and those external disturbances have a negative impact on control performance [47]. Besides, Shi *et al.* [48] proposed the output-feedback control for time-delay systems with PPF constraints. In response to the explosion of the complex problem, a dynamic surface control technique has been proposed by Zhai *et al.* [49]. Nonetheless, the PPF constraints with CFC are not considered for pneumatic active suspension.

Based on the aforementioned discussion, we propose a new active suspension system using a pneumatic spring in this research. Although pneumatic actuators can meet the requirements of flexible suspension, controlling the stability of the sprung mass within a small predefined boundary remains a challenge because of their parametric uncertainties and external disturbances. As we know that PPF constraints can guarantee the vertical displacement for the active suspension, but the unknown parameters may cause the problem of singularity and instability. Besides, actuator saturation usually leads to the performance degradation of the pneumatic actuator, so the system design becomes more difficult without knowledge of control directions. In this study, a novel control is established for ASSs with PPF constraint while the result did not require prior knowledge of control gains. By using neural networks, the unknown parameters are compensated to guarantee the performance of the pneumatic suspension. Furthermore, a command filtered control has been studied to solve the explosion of complexity in traditional backstepping controllers. Command filtered control combined with PPF is proposed not only to handle the explosion of complexity problem in the traditional backstepping techniques but also to guarantee the tracking error of sprung mass displacement

does not violate the constraint boundaries. The Levant differentiators are introduced in the CFC control scheme to compute the derivative approximation of the virtual control signals and the compensating signals are then designed to eliminate the errors caused by the command filters. To design the CFC technique with input saturation, the Gaussian error function is employed to express the saturation nonlinearity as a continuous differentiable form. In addition, the Nussbaum gain function is applied to solve the difficulty of the control design due to the uncertain control directions of active suspension. Based on the Lyapunov stability analysis, the control scheme can ensure that all the signals are semi-global uniformly ultimately bounded. The main contributions of this paper can be summarized as follows

1. Adaptive neural command filtered backstepping control is proposed for the pneumatic active suspension which considers the problem of actuator saturation and unknown control direction.

2. RBFNNs are developed to approximate the parametric uncertainties of the pneumatic spring and the unknown various loads of passengers in the nonlinear ASSs.

The rest of this paper is organized as follows. System description of the pneumatic quarter car model is given in Section II. Adaptive neural command filtered control and the system stability are presented in Section III. Besides, to demonstrate the effectiveness of the proposed control, the comparative simulation results are provided in section IV. Finally, Section V gives some conclusions.

II. SYSTEM DESCRIPTION AND NOTATIONS

A. NONLINEAR QUARTER CAR MODEL

The quarter car model with pneumatic spring is designed as shown in Fig. 1. In this design, the chassis is affected by external disturbances that cause continuous excitations to the passengers. The suspension system is designed to dissipate this vibration for the passenger comfort. The dynamic equations of active suspension are demonstrated as

$$\begin{aligned} &m_s\ddot{z}_s + F_s(z_s, z_u, t) + F_d(\dot{z}_s, \dot{z}_u, t) = F_u \\ &m_u\ddot{z}_u - F_s(z_s, z_u, t) - F_d(\dot{z}_s, \dot{z}_u, t) \\ &\qquad + F_{st}(z_u, z_r, t) + F_{dt}(\dot{z}_u, \dot{z}_r, t) = -F_u \end{aligned} \tag{1}$$

where m_s and m_u denote sprung mass and unsprung mass, respectively. The unsprung mass represents an assembly of the vehicle axis and wheel while the sprung mass is the total weight of the chassis and passengers.

These above forces are created by the stiffness of pneumatic spring, mechanical springs, damper, and tire, which can be expressed as $F_s(z_s, z_u, t) = (k_s + k_a)(z_s - z_u)$, $F_d(\dot{z}_s, \dot{z}_u, t) = c_a(\dot{z}_s - \dot{z}_u)$, $F_{st}(z_u, z_r, t) = k_t(z_u - z_r)$, $F_{dt}(\dot{z}_u, \dot{z}_r, t) = c_t(\dot{z}_u - \dot{z}_r)$, where z_s and z_u determine the position of the sprung mass and unsprung mass, z_r presents the road profile; k_s, c_a are the stiffness coefficient and damping coefficient of active suspension; and k_t, c_t represent the stiffness and the damping coefficient of the tire.

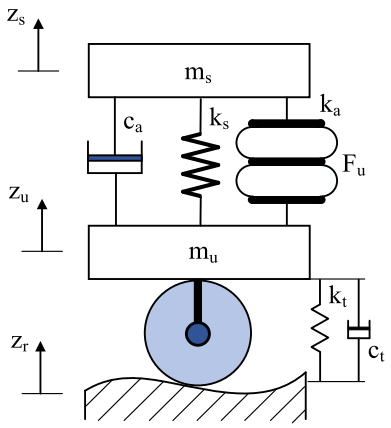

FIGURE 1. Pneumatic active suspension model.

The tire force which depends on the road holding condition is expressed by the equation (2), where g denotes the gravitational acceleration [50].

$$F_t = \begin{cases} F_{st} + F_{dt}, & if\ F_{st} + F_{dt} < (m_s + m_u)\, g \\ 0, & if\ F_{st} + F_{dt} \geq (m_s + m_u)\, g \end{cases} \tag{2}$$

Define the systems state variables: $x_1 = z_s$, $x_2 = \dot{z}_s$, $x_3 = z_u$, $x_4 = \dot{z}_u$, the state space form of active suspension can be written as follows

$$\begin{aligned} \dot{x}_1 &= x_2 \\ \dot{x}_2 &= \frac{1}{m_s}\left[-F_s(x_1, x_3, t) - F_d(x_2, x_4, t) + F_u\right] \\ \dot{x}_3 &= x_4 \\ \dot{x}_4 &= \frac{1}{m_u}\left[\begin{array}{r} -F_{st}(x_3, z_r, t) - F_{dt}(x_4, \dot{z}_r, t) \\ +F_s(x_1, x_3, t) + F_d(x_2, x_4, t) - F_u \end{array}\right] \end{aligned} \tag{3}$$

To provide the active force for the active suspension system, an air below is installed between the sprung and unsprung masses. The active fore of air bellow F_u is calculated by the following formula

$$F_u = A_{\text{as}} P_{as} \tag{4}$$

where A_{as} represents the working area and P_{as} is the internal pressure of the air bellow.

Because the aerodynamic properties of the air bellow are caused by the action of the twisted-wire rubber material under the effect of external forces, there is a challenge to describe the absolute mathematical model. Therefore, the nonlinear dynamic model can be investigated by [2]

$$\dot{P}_{as} = \frac{\gamma RT}{v_{as}}\left(a_0 q_{as} - \frac{P_{as} A_{as}(x_2 - x_4)}{RT}\right) \tag{5}$$

where R is the ideal gas constant, γ represents the polytropic index, T denotes the air temperature, q_{as} is the area-normalized mass flow rate, and a_0 denotes the orifice open area of the solenoid valve.

The air bellow volume v_{as} depends on the relative motion between the sprung mass and unsprung mass

$$v_{as} = A_{as}\left(z_{as0} + x_1 - x_3\right) \tag{6}$$

where z_{as0} denotes the initial altitude of the air bellow.

Assumption 1: The spool position is proportional to the signal applied to the control valve. Hence, the valve dynamics can be ignored in the system model, and the orifice open area a_0 of the servo valve can be described by

$$a_0 = \sigma_{sv} u \tag{7}$$

where σ_{sv} is the coefficient factor of the servo valve and u is the control signal of supply voltage.

Using (6) and (7), we can write the dynamic model of air bellow (5) as follows

$$\dot{P}_{as} = \frac{\gamma RT}{A_{as}\left(z_{as0} + x_1 - x_3\right)}\left(\sigma_{sv} q_{as} u - \frac{P_{as} A_{as}\left(x_2 - x_4\right)}{RT}\right) \tag{8}$$

Define the new state variable $x_5 = (A_{as}/m_s)P_{as}$, we obtain

$$\dot{x}_5 = \frac{\gamma RT}{m_s\left(z_{as0} + x_1 - x_3\right)}\sigma_{sv} q_{as} u - \frac{\gamma}{\left(z_{as0} + x_1 - x_3\right)} x_5\left(x_2 - x_4\right) \tag{9}$$

B. PROBLEM FORMULATION

The nonlinear pneumatic stiffness k_a exists in the air bellow, depending on the internal pressure and the axial displacements. Some previous studies have examined this stiffness based on the thermodynamic theory [51] but it cannot be applied to the control design process because of different working conditions. In this study, the air spring stiffness is considered as an uncertain parameter and then compensated by NNs. Therefore, we can define the unknown continuous function as follows

$$d\left(t\right) = \frac{1}{m_s}\left[-k_a(x_1 - x_3)\right] \tag{10}$$

Besides, the pressure of air bellow is a high nonlinearity model as it is affected by external disturbances, payload variations, and unmodeled dynamics. Thus, the dynamic model (9) should consider the parameter deviations which are lumped to the unmodeled terms. The state-space form of the quarter car ASSs must be extended using the pneumatic stiffness and unmodeled parameters of air spring as follows

$$\begin{aligned}
\dot{x}_1 &= x_2 \\
\dot{x}_2 &= x_5 + \frac{1}{m_s}\left[-k_s(x_1 - x_3) - c_a(x_2 - x_4)\right] + d\left(t\right) \\
\dot{x}_3 &= x_4 \\
\dot{x}_4 &= \frac{1}{m_u}\left[\begin{array}{l} -k_t(x_3 - z_r) - c_t(x_4 - \dot{z}_r) \\ \quad +k_s(x_1 - x_3) + c_a(x_2 - x_4) - m_s x_5 \end{array}\right] \\
&\quad - \frac{m_s}{m_u} d\left(t\right) \\
\dot{x}_5 &= \frac{\gamma RT}{m_s\left(z_{as0} + x_1 - x_3\right)}\sigma_{sv} q_{as} u \\
&\quad - \frac{\gamma}{\left(z_{as0} + x_1 - x_3\right)} x_5\left(x_2 - x_4\right) + p\left(t\right)
\end{aligned} \tag{11}$$

where $p\left(t\right)$ is the time-varying modeling error of air bellow pressure.

Assumption 2: $d\left(t\right)$ and $p\left(t\right)$ are the unknown bounded time-varying disturbances. Therefore, there are two constants $\bar{d}\left(t\right)$ and $\bar{p}\left(t\right)$ satisfying $\left|d\left(t\right)\right| \le \bar{d}\left(t\right)$ and $\left|p\left(t\right)\right| \le \bar{p}\left(t\right)$.

Assumption 3: Due to the limitations of the mechanical structure and physical performance, the mass of the vehicle body is limited by $m_{s\min} < m_s < m_{s\max}$, where $m_{s\min}$ and $m_{s\max}$ are the lower and upper limits.

To ensure the ride comfort, the air bellow is used to create the active force that isolates the external vibrations in the suspension design. However, because of the limitations of the pneumatic actuator, the dissipation of vibration will be considered during the control design process. Thus, the problem of input saturation is solved for pneumatic active suspension in this study. The control signal u that is the output of the saturation actuator can be assumed by

$$u = sat\left(v\right) = \begin{cases} v, & |v| < u_B \\ u_B sign\left(v\right), & |v| \ge u_B \end{cases} \tag{12}$$

where v is the actual input signal and u_B is the known bound of u.

It can be seen that the relationship between u and v in equation (12) is a saturation nonlinearity which has sharp corners as $|v| = u_B$. Thus, it cannot be directly applied to the backstepping control. To overcome this limitation, a Gaussian error function is employed to express the saturation nonlinearity that can be used for the control design.

Definition 1 [34]: Gauss error function $erf\left(x\right)$ is described by a nonelementary function of sigmoid shape

$$erf\left(x\right) = \frac{2}{\sqrt{\pi}}\int_0^x e^{-t^2} dt \tag{13}$$

Remark 1: Error function $erf\left(x\right)$ is a continuously differentiable function, it has real value and has no singularity (except that at infinity).

To facilitate the control design later, the output signal u is defined by [52]

$$u = h_v v + d\left(v\right) \tag{14}$$

where the smooth function h_v is used to approximate the saturation nonlinearity and $d\left(v\right)$ is bounded by $\left|d(v)\right| \le \Delta$.

Control objectives: The control scheme is designed to meet three requirements of active suspension

1. *Ride comfort:* The controller is proposed to dissipate continuous excitations and guarantee the vertical displacement of sprung mass within the bounded constraints.
2. *Handling stability:* The oscillation space cannot exceed the limited range of suspension displacement. To meet this requirement, the relative suspension deflection (RSD) must be ensured to be less than 1.

$$RSD = \frac{z_s - z_u}{z_R} \tag{15}$$

where z_R which is called rattle space is defined as the distance between the tire and chassis at rest position.

3. *Road holding:* The dynamic tire load must be limited to ensure that the tire is always kept in contact with the road profile. It means that the relative tire fore (RTF) is kept smaller than 1.

$$RTF = \frac{F_t}{(m_s + m_u)\, g} \tag{16}$$

Remark 2: Although some advance controllers have been proposed for the active suspension to provide passenger comfort by limiting the sprung mass displacement, the objective of handling stability cannot be guaranteed simultaneously because they conflict with each other. The proposed control in this study can improve all three objectives of active suspension and ensure that the tracking error of sprung mass displacement does not violate the PPF constraints.

C. NOTATIONS

In this study, a norm of vector x is defined by $\|x\| = \sqrt{x^T x}$. The estimate of generic constant quantity θ is indicated by $\hat{\theta}$. Moreover, the estimation error and its time derivative are $\tilde{\theta} = \theta - \hat{\theta}$ and $\dot{\tilde{\theta}} = -\dot{\hat{\theta}}$, respectively. Some symbols and their descriptions are given in Table 1.

TABLE 1. Symbols.

Symbol	Description
$N(\zeta)$	Nussbaum-type function
ξ_i	Center of the Gaussian functions
σ_i	Width of the Gaussian functions
ω_i	Compensating signals
$\rho(t)$	Prescribed performance function
k_1, k_2, k_3	Control design parameters
p	Adaptive law parameter
$S(X)$	Gaussian function vector
$\eta(X)$	Approximation error
W	Weight vector
L_{i1}, L_{i2}	Levant differentiators

III. ADAPTIVE NEURAL COMMAND FILTERED CONTROL WITH PRESCRIBED PERFORMANCE

A. SOME DEFINITIONS AND LEMMAS

To guarantee the vertical displacement of sprung mass within boundary constraints, the proposed control design will focus on the dynamic equations of the sprung mass as follows

$$\begin{aligned}
\dot{x}_1 &= x_2 \\
\dot{x}_2 &= x_5 + \frac{1}{m_s}\left[-k_s(x_1 - x_3) - c_a(x_2 - x_4)\right] + d\,(t) \\
\dot{x}_5 &= \frac{\gamma RT}{m_s\,(z_{as0} + x_1 - x_3)}\sigma_{sv} q_{as} u - \frac{\gamma}{(z_{as0} + x_1 - x_3)} \\
&\quad \times x_5\,(x_2 - x_4) + p\,(t)
\end{aligned} \tag{17}$$

By setting $f_2 = (1/m_s)[-k_s(x_1 - x_3) - c_a(x_2 - x_4)]$, $g_2 = 1$, $f_3 = [-\gamma/(z_{as0} + x_1 - x_3)]x_5(x_2 - x_4)$, $g_3 = \{\gamma RT/[m_s(z_{as0} + x_1 - x_3)]\}\sigma_{sv} q_{as}$, we can rewrite (17) as follows

$$\begin{aligned}
\dot{x}_1 &= x_2 \\
\dot{x}_2 &= f_2 + g_2 x_5 + d\,(t) \\
\dot{x}_5 &= f_3 + g_3 u + p\,(t)
\end{aligned} \tag{18}$$

In the above equation (18), it can be seen that f_2 and f_3 are unknown smooth functions because the system state x_4 is not considered in the control design. In real suspension, the sprung mass m_s is an unknown parameter, depending on different passenger masses. Besides, the damping properties of air bellow cannot be accurately described and are often ignored in the active suspension.

Remark 3: The nonlinear smooth function g_3 contains the unknown parameter m_s and depends on the relative values of x_1 and x_3. Thus, the control directions are specified as the sign of variable control gain g_3.

Assumption 4: The unknown function g_3 is bounded and there is a known positive constant satisfying $|g_3| \le \upsilon$.

Lemma 1 [26]: The RBFNNs can approximate any unknown continuous function $f\,(X)$

$$f\,(X) = W_h^T S\,(X) + \eta\,(X) \tag{19}$$

where $W = [w_1, w_2, \ldots, w_n]^T \in R^n$ denote the weight vector, $S\,(X) = [s_1\,(X), s_2\,(X), \ldots, s_n\,(X)]^T$ is the Gaussian function vector, $\eta\,(X)$ illustrates the approximation error, $n > 1$ is the node number of RBFNNs, and X represents the input vector.

The Gaussian functions are described by

$$S_i(\mathrm{X}) = \exp\left(-\frac{\|X - \xi_i\|^2}{\sigma_i^2}\right), \quad i = 1, 2, \ldots, \mathrm{n} \tag{20}$$

where ξ_i and σ_i are the center and width of the Gaussian functions.

There exists an arbitrary positive constant $\lambda > 0$ such that $\left|W_h^T S(X) - f(X)\right| \le \lambda$ [53].

Lemma 2 [37]: The Nussbaum gain technique is used to handle the unknown sign of variable control coefficient g_3. Any continuous function $N\,(\zeta)$ is called a Nussbaum-type function if is satisfied

$$\begin{aligned}
\lim_{s\to\infty} sup \frac{1}{s}\int_0^s N\,(\zeta)d\zeta &= +\infty \\
\lim_{s\to\infty} inf \frac{1}{s}\int_0^s N\,(\zeta)d\zeta &= -\infty
\end{aligned} \tag{21}$$

Some Nussbaum functions can be recommended, such as: $N\,(\zeta) = \zeta^2 \cos(\zeta), N\,(\zeta) = \zeta^2 \sin(\zeta), N\,(\zeta) = e^{\zeta^2}\cos\left(\zeta\pi/2\right)$. In this study, the function $N\,(\zeta) = \zeta^2 \cos(\zeta)$ is used.

Lemma 3 [54]: Let V and ζ be smooth functions defined on $[0, t_f)$ with $V(t) \ge 0$. If the following inequality holds on $t \in [0, t_f)$

$$V\,(t) \le c_0 + e^{-c_1 t}\int_0^t (g\,(\tau)N\,(\zeta) + 1)\dot{\zeta} e^{c_1 \tau} d\tau \tag{22}$$

where $c_0, c_1 > 0$ are the constant parameters, then $V(t)$, $\zeta(t)$, and $\int_0^t g(\tau) N(\zeta)\dot{\zeta} e^{c_1\tau} d\tau$ must be bounded on $[0, t_f)$.

Lemma 4 [55]: The command filters of CFC are defined based on Levant differentiator as follows

$$\begin{aligned} \dot{L}_{i1} &= -R_1 |L_{i1} - \alpha_{i-1}|^{\frac{1}{2}} sign(L_{i1} - \alpha_{i-1}) + L_{i2} \\ \dot{L}_{i2} &= -R_2 sign\left(L_{i2} - \dot{L}_{i1}\right), \quad i = 2, 3 \end{aligned} \tag{23}$$

where $x_{i,c} = L_{i1}$ and $\dot{x}_{i,c} = \dot{L}_{i1}$ are the output of each filter used to define tracking error $e_i = x_i - x_{ic}$. Each command filter is designed to compute x_{ic} and $\dot{x}_{ic}$ without differentiation. The design parameters of differentiators are chosen by R_1 and R_2 while α_{i-1} are the virtual control at each step. If the input signal α_{i-1} and their derivatives are bounded and satisfied $|\dot{\alpha}_{i-1}| \leq \mu_1$ and $|\ddot{\alpha}_{i-1}| \leq \mu_2$ in a finite time with $\mu_1 > 0$, $\mu_2 > 0$, the following inequality holds

$$|L_{i1} - \alpha_{i-1}| \leq \mu \tag{24}$$

where $\mu > 0$ is a positive constant. The finite-time error convergence characteristics of the Levant's differentiators were proved in [55] and [56].

Remark 4: The Levant differentiators can improve the limitations of traditional CFC by providing a precise filter of the input signals to obtain the differential signals and guarantee the convergence of the filter in a finite-time.

Lemma 5 [20]: It can be seen that the tracking errors caused by command filters can lead to an increase in system errors. To eliminate the effect of the errors caused by command filters, the compensating signals ω_i for command filtered control are selected by

$$\begin{aligned} \dot{\omega}_1 &= -k_1\omega_1 + g_1\omega_2 + g_1(x_{2c} - \alpha_1) \\ \dot{\omega}_i &= -k_i\omega_i - g_{i-1}\omega_{i-1} + g_i\omega_{i+1} + g_i\left(x_{(i+1)c} - \alpha_i\right) \\ \dot{\omega}_n &= 0 \end{aligned} \tag{25}$$

where $\omega_i(0) = 0$ for $t \in [0, T_1]$, and k_i are designed positive constants.

According to [21], the compensating signals are bounded by

$$\|\omega_i(t)\| \leq \frac{\upsilon\mu}{2k_0}\left(1 - e^{-2k_0(t-T_1)}\right) \tag{26}$$

where $k_0 = (1/2)\, min\,(k_i)$

B. PRESCRIBED PERFORMANCE CONSTRAINT

To guarantee the stability of the chassis does not violate the boundaries in vertical displacement, a PPF constraint is introduced into the control design. First, let the tracking error of the system state x_1 be defined as

$$e_1 = x_1 - x_d \tag{27}$$

where x_d is the desired position trajectory.

Definition 2 [40]: The PPF constraint is chosen by a positive smooth function as follows

$$\rho(t) = (\rho_0 - \rho_\infty) e^{-\varphi t} + \rho_\infty \tag{28}$$

where $\varphi > 0$ denotes the convergence rate, ρ_0 is the initial value, and ρ_∞ indicates the allowable steady-state error, which must be chosen to satisfy the initial conditions $\lim_{t\to 0} \rho(t) = \rho_0 > 0$, $\lim_{t\to\infty} \rho(t) = \rho_\infty > 0$, and $\rho_0 > \rho_\infty$.

From (28), the tracking error of sprung mass displacement can be guaranteed by the following inequality

$$-\underline{\kappa}\rho(t) < e_1 < \bar{\kappa}\rho(t), \quad t > 0 \tag{29}$$

where $\underline{\kappa}, \bar{\kappa} > 0$ are the positive parameters chosen by the designers.

Remark 5: Based on (28) and (29), the lower bound of the undershoot is defined by $-\underline{\kappa}\rho(0)$ while $\bar{\kappa}\rho(0)$ serves as the upper bound of the maximum overshoot. By choosing the appropriate design parameters $\underline{\kappa}$, $\bar{\kappa}$, ρ_0, ρ_∞, φ, the steady-state performance of the system can be guaranteed.

To design the control scheme with PPF constraint, an output transformation is used to construct the prescribed performance boundary into an equality form. For this purpose, a smooth and strictly increasing function $S(z_1)$ is introduced as follows [40].

$$S(z_1) = \frac{\bar{\kappa}e^{z_1} - \underline{\kappa}e^{-z_1}}{e^{z_1} + e^{-z_1}} \tag{30}$$

Furthermore, the function $S(z_1)$ satisfies

1. $-\underline{\kappa} < S(z_1) < \bar{\kappa}$
2. $\lim_{z_1\to\infty} S(z_1) = \bar{\kappa}$, $\lim_{z_1\to-\infty} S(z_1) = -\underline{\kappa}$

Then, the performance condition (29) can be transferred as follows

$$e_1 = \rho(t) S(z_1) \tag{31}$$

Because $S(z_1)$ is strictly monotonically increasing and PPF constraint was chosen to satisfy $\rho(t) > \rho_\infty > 0$, the inverse transfer function z_1 can be expressed by

$$z_1 = S^{-1}\left(\frac{e_1}{\rho(t)}\right) \tag{32}$$

Set $\beta = e_1/\rho(t)$, we can write the transform function of z_1 as follows

$$z_1 = \frac{1}{2}\ln\left(\frac{\beta + \underline{\kappa}}{\bar{\kappa} - \beta}\right) \tag{33}$$

Lemma 6 [57]: Based on the above analysis, the system state (17) is transformed by the smooth function $S(z_1)$ of equation (30) and the stability of the signal e_1 can guarantee the regulation of x_1 according to the prescribed performance constraint (29).

Remark 6: PPF constraint (28) and error transform $S(z_1)$ are proposed for the control design process by choosing the control parameters $\rho_0, \rho_\infty, \varphi, \underline{\kappa}, \bar{\kappa}$. Since the parameters $\rho_0, \underline{\kappa}, \bar{\kappa}$ are selected so that the initial condition $-\underline{\kappa}\rho(0) < x_1(0) < \bar{\kappa}\rho(0)$ satisfies and z_1 can be restricted within the boundaries, the condition $-\underline{\kappa} < S(z_1) < \bar{\kappa}$ is held. Therefore, the control problem (17) under the condition $-\underline{\kappa}\rho(t) < x_1(t) < \bar{\kappa}\rho(t)$ is guaranteed.

C. ADAPTIVE NEURAL COMMAND FILTERED BACKSTEPPING CONTROL

In this section, an adaptive neural command filtered scheme is designed based on a modified backstepping algorithm. The unknown parameters are approximated by the NNs while the PPF is introduced to ensure the tracking error of sprung mass displacement within the boundary constraints. Besides, the stability of the proposed control scheme is demonstrated by the Lyapunov theorem. The controller diagram can be described in Fig. 2.

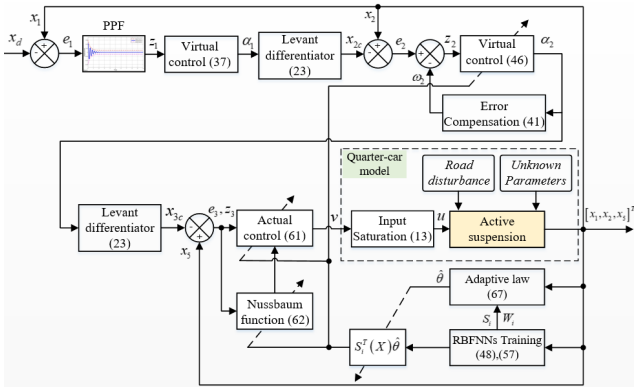

FIGURE 2. Block diagram of Adaptive NNs CFC with PPF.

Step 1: Identify the inverse transfer function z_1 with PPF in section III.B

Step 2: Design the virtual control α_1

The derivative of z_1 is given by using (33) as follows

$$\dot{z}_1 = \frac{1}{2}\left(\frac{1}{\beta+\underline{\kappa}} - \frac{1}{\beta-\bar{\kappa}}\right)\left(\frac{\dot{x}_1}{\rho} - \frac{x_1\dot{\rho}}{\rho^2}\right) = \varsigma\left(x_2 - \frac{x_1\dot{\rho}}{\rho}\right) \tag{34}$$

where $\varsigma = \frac{1}{2\rho}\left(\frac{1}{\beta+\kappa} - \frac{1}{\beta-\bar{\kappa}}\right)$

A candidate Lyapunov function is chosen as $V_1 = (1/2)\, z_1^2$. Then, the time derivative of V_1 is obtained by

$$\dot{V}_1 = z_1\dot{z}_1 \tag{35}$$

In this step, the control algorithm is based on the basis of the backstepping algorithm, we have

$$\dot{V}_1 = z_1\varsigma\left(z_2 + \alpha_1 - \frac{x_1\dot{\rho}}{\rho}\right) \tag{36}$$

The virtual control α_1 is selected as follows

$$\alpha_1 = \frac{x_1\dot{\rho}}{\rho} - \varsigma^{-1}k_1 z_1 \tag{37}$$

Substituting (37) into (36) leads to

$$\dot{V}_1 = -k_1 z_1^2 + z_1\varsigma z_2 \tag{38}$$

Step 3: Design the virtual control α_2

The tracking error of x_2 is designed based on command filtered backstepping theory

$$e_2 = x_2 - x_{2c} \tag{39}$$

where x_{2c} is the output signal of the command filter while the virtual controller α_1 goes through the filter.

In this step, the compensated tracking error is redefined based on the theory of command filtered backstepping as follows

$$z_2 = e_2 - \omega_2 \tag{40}$$

The error compensation is proposed based on (25)

$$\dot{\omega}_2 = -k_2\omega_2 + g_2\omega_3 + g_2\left(x_{3c} - \alpha_2\right) \tag{41}$$

Choose the candidate Lyapunov function V_2

$$V_2 = V_1 + \frac{1}{2}z_2^2 \tag{42}$$

Taking the derivative of V_2, we have

$$\dot{V}_2 = -k_1 z_1^2 + z_2\left(z_1\varsigma + \dot{z}_2\right) \tag{43}$$

Using (39), (40), and (41), we can write (43) as follows

$$\dot{V}_2 = -k_1 z_1^2 + z_2\left(z_1\varsigma + \dot{x}_2 - \dot{x}_{2c} - \dot{\omega}_2\right) \tag{44}$$

$$\dot{V}_2 = -k_1 z_1^2 + z_2\begin{pmatrix} z_1\varsigma + f_2 + g_2 x_5 + d\left(t\right) - \dot{x}_{2c} \\ +k_2\omega_2 - g_2\omega_3 - g_2 x_{3c} + g_2\alpha_2 \end{pmatrix} \tag{45}$$

Choose the virtual control α_2

$$\alpha_2 = \frac{1}{g_2}\left(-z_1\varsigma - \frac{z_2 S_2^T S_2\hat{\theta}}{2r_2^2} + \dot{x}_{2c} - z_2 - k_2 e_2\right) \tag{46}$$

where r_2 is a positive constant, $\hat{\theta}$ denotes adaptive law which is determined later.

Then, the equation (45) will be written as

$$\dot{V}_2 = -k_1 z_1^2 + z_2\begin{pmatrix} f_2 + g_2 x_5 + d\left(t\right) + k_2\omega_2 - g_2\omega_3 \\ -g_2 x_{3c} - \frac{z_2 S_2^T S_2\hat{\theta}}{2r_2^2} - z_2 - k_2 e_2 \end{pmatrix} \tag{47}$$

According to (47), the virtual control signal is difficult to be designed because of the unknown function f_2. In this step, f_2 will be approximated by NNs according to Lemma 1.

$$f_2\left(X_2\right) = W_2^T S_2\left(X_2\right) + \eta_2\left(X_2\right) \tag{48}$$

It can be seen from (17), the unknown function $f\left(X_2\right)$ is related to these variables x_1 and x_2, so we choose $X_2 = [x_1, x_2]^T$, and η_2 is the approximation error satisfying $|\eta_2| < \lambda_2$. Basing on Young's inequality theorem and Assumption 2, we have

$$\begin{aligned} z_2 f_2\left(X_2\right) &= z_2\left(W_2^T S_2 + \eta_2\right) \\ &\le \frac{1}{2r_2^2}z_2^2\left\|W_2\right\|^2 S_2^T S_2 + \frac{1}{2}r_2^2 + \frac{1}{2}z_2^2 + \frac{1}{2}\lambda_2^2 \end{aligned} \tag{49}$$

$$z_2 d\left(t\right) \le \frac{1}{2}z_2^2 + \frac{1}{2}\bar{d}^2 \tag{50}$$

Rewrite equation (47) using (49) and (50), we have

$$\dot{V}_2 \leq -k_1 z_1^2 - k_2 z_2^2 + \frac{1}{2r_2^2} z_2^2 \left(\|W_2\|^2 - \hat{\theta} \right) S_2^T S_2 + g_2 z_2 z_3 + \frac{1}{2} r_2^2 + \frac{1}{2} \lambda_2^2 + \frac{1}{2} \bar{d}^2 \quad (51)$$

Step 4: Design the control signal u

In this step, the tracking error of x_5 is considered by

$$e_3 = x_5 - x_{3c} \quad (52)$$

where x_{3c} is the output signal of the command filter.

The compensated tracking error is defined as follows

$$z_3 = e_3 - \omega_3 \quad (53)$$

The error compensation is suggested by (25)

$$\dot{\omega}_3 = 0 \quad (54)$$

Choose the Lyapunov function V_3 as follows

$$V_3 = V_2 + \frac{1}{2} z_3^2 \quad (55)$$

Then, the derivative of V_3 can be transformed into

$$\dot{V}_3 = -k_1 z_1^2 - k_2 z_2^2 + \frac{1}{2r_2^2} z_2^2 \left(\|W_2\|^2 - \hat{\theta} \right) S_2^T S_2 + \frac{1}{2} r_2^2 + \frac{1}{2} \lambda_2^2 + \frac{1}{2} \bar{d}^2 + g_2 z_2 z_3 + z_3 \left(f_3 + g_3 u + p(t) - \dot{x}_{3c} \right) \quad (56)$$

Similar to step 3, the unknown function $f_3(X_3) = (f_3 + g_2 z_2 - \dot{x}_{3c})$ can be approximated by NNs.

$$f_3(X_3) = W_3^T S_3(X_3) + \eta_3(X_3) \quad (57)$$

where $X_3 = [x_1, x_2, x_5]^T$. Let η_3 be the approximation error satisfying $|\eta_3| < \lambda_3$, and apply Young's inequality theorem and Assumption 2, we obtain

$$z_3 f_3(X_3) \leq \frac{1}{2r_3^2} z_3^2 \|W_3\|^2 S_3^T S_3 + \frac{1}{2} r_3^2 + \frac{1}{2} z_3^2 + \frac{1}{2} \lambda_3^2 \quad (58)$$

$$z_3 p(t) \leq \frac{1}{2} z_3^2 + \frac{1}{2} \bar{p}^2 \quad (59)$$

where r_3 is the positive control parameter.

Using the form of real control law (14) and substituting equations (58) and (59) into (56), we can write the derivative of V_3 as follows

$$\dot{V}_3 \leq -k_1 z_1^2 - k_2 z_2^2 + \frac{1}{2r_2^2} z_2^2 \left(\|W_2\|^2 - \hat{\theta} \right) S_2^T S_2 + \frac{1}{2} r_2^2 + \frac{1}{2} \lambda_2^2 + \frac{1}{2} \bar{d}^2 + \frac{1}{2} r_3^2 + \frac{1}{2} \lambda_3^2 + \frac{1}{2} \bar{p}^2 + z_3^2 + z_3 \left(g_3 (h_v v + d(v)) + \frac{1}{2r_3^2} z_3 \|W_3\|^2 S_3^T S_3 \right) \quad (60)$$

Because the control coefficient is unknown, the Nussbaum function is introduced to handle the problem of unknown control directions. Hence, the actual input signal v can be designed by

$$v = N(\zeta) \left[k_3 z_3 + \frac{1}{2r_3^2} z_3 S_3^T S_3 \hat{\theta} \right] \quad (61)$$

where $N(\zeta)$ is Nussbaum-type function and the smooth function ζ is chosen as

$$\dot{\zeta} = k_3 z_3^2 + \frac{1}{2r_3^2} z_3^2 S_3^T S_3 \hat{\theta} \quad (62)$$

Apply Young's inequality theorem, we can write

$$z_3 g_3 d(v) \leq \frac{1}{2} z_3^2 + \frac{1}{2} g_3^2 \Delta^2 \quad (63)$$

Then, (60) can be rewritten using (61), (62), and (63) as follows

$$\dot{V}_3 \leq -\sum_{i=1}^{2} k_i z_i^2 - \left(k_3 - \frac{3}{2} \right) z_3^2 + \sum_{i=2}^{3} \frac{1}{2r_i^2} z_i^2 \left(\|W_i\|^2 - \hat{\theta} \right) S_i^T S_i + \frac{1}{2} \sum_{i=2}^{3} r_i^2 + \frac{1}{2} \sum_{i=2}^{3} \lambda_i^2 + \frac{1}{2} \bar{d}^2 + \frac{1}{2} \bar{p}^2 + \frac{1}{2} g_3^2 \Delta^2 + (g_3 h_v N(\zeta) + 1) \dot{\zeta} \quad (64)$$

Consider the Lyapunov function V

$$V = V_3 + \frac{1}{2m} \tilde{\theta}^2 \quad (65)$$

where m is the positive parameter and $\tilde{\theta} = \theta - \hat{\theta}$ is the estimation error. By choosing $\theta = max \left\{ \|W_2\|^2, \|W_3\|^2 \right\}$ for the time derivative of V, we have

$$\dot{V} \leq -\sum_{i=1}^{2} k_i z_i^2 - \left(k_3 - \frac{3}{2} \right) z_3^2 + \frac{1}{m} \tilde{\theta} \left(\sum_{i=2}^{3} \frac{m}{2r_i^2} z_i^2 S_i^T S_i - \dot{\hat{\theta}} \right) + \frac{1}{2} \bar{d}^2 + \frac{1}{2} \sum_{i=2}^{3} r_i^2 + \frac{1}{2} \sum_{i=2}^{3} \lambda_i^2 + \frac{1}{2} \bar{p}^2 + \frac{1}{2} g_3^2 \Delta^2 + (g_3 h_v N(\zeta) + 1) \dot{\zeta} \quad (66)$$

The adaptive law is designed as follows

$$\dot{\hat{\theta}} = \sum_{i=2}^{3} \frac{m}{2r_i^2} z_i^2 S_i^T S_i - q \hat{\theta} \quad (67)$$

where q is the design parameter.

Theorem: Consider the pneumatic active suspension system (17) satisfying Assumptions 1 - 4, the virtual controllers (37), (46), actual control (61), and adaptation law (67) are designed. The proposed control can ensure that all system signals are semi-globally uniformly ultimately bounded. This leads to the estimation errors converging to a small set around zero asymptotically. It means that the sprung mass displacement is guaranteed within the PPF constraint.

Proof: Applying Young's inequality, we have

$$\frac{q}{m}\tilde{\theta}\hat{\theta} \leq \frac{q}{2m}\theta^2 - \frac{q}{2m}\tilde{\theta}^2 \tag{68}$$

Therefore, we can rewrite (66) using (67) and (68) as follows

$$\begin{aligned}\dot{V} \leq & -\sum_{i=1}^{2} k_i z_i^2 - \left(k_3 - \frac{3}{2}\right) z_3^2 + \frac{1}{2}\sum_{i=2}^{3} r_i^2 + \frac{1}{2}\sum_{i=2}^{3}\lambda_i^2 \\ & + \frac{q}{2m}\theta^2 \\ & - \frac{q}{2m}\tilde{\theta}^2 + \frac{1}{2}\bar{d}^2 + \frac{1}{2}\bar{p}^2 + \frac{1}{2}g_3^2\Delta^2 + \left(g_3 h_v N(\zeta) + 1\right)\dot{\zeta}\end{aligned} \tag{69}$$

Because the unknown function g_3 is bounded under Assumption 4, we can write the third part of equation (63) as follows $g_3^2\Delta^2 \leq \upsilon^2\Delta^2$. Hence, the equation (69) can be written as

$$\begin{aligned}\dot{V} \leq & -\sum_{i=1}^{2} k_i z_i^2 - \left(k_3 - \frac{3}{2}\right) z_3^2 - \frac{q}{2m}\tilde{\theta}^2 + \frac{1}{2}\sum_{i=2}^{3} r_i^2 + \frac{1}{2}\sum_{i=2}^{3}\lambda_i^2 \\ & + \frac{1}{2}\bar{d}^2 + \frac{1}{2}\bar{p}^2 + \frac{q}{2m}\theta^2 + \frac{1}{2}\upsilon^2\Delta^2 + \left(g_3 h_v N(\zeta) + 1\right)\dot{\zeta}\end{aligned} \tag{70}$$

By setting $\Phi = min\left\{2k_1, 2k_2, 2\left(k_3 - \frac{3}{2}\right), q\right\}$ and $\Xi = \frac{1}{2}\sum_{i=2}^{3} r_i^2 + \frac{1}{2}\sum_{i=2}^{3}\lambda_i^2 + \frac{1}{2}\bar{d}^2 + \frac{1}{2}\bar{p}^2 + \frac{q}{2m}\theta^2 + \frac{1}{2}\upsilon^2\Delta^2$, we can obtain

$$\dot{V} \leq -\Phi V + \Xi + \left(g_3 h_v N(\zeta) + 1\right)\dot{\zeta} \tag{71}$$

Multiplying (71) by $e^{\Phi t}$ on both sides and then integrating, it leads to

$$e^{\Phi t}\dot{V} + \Phi e^{\Phi t} V \leq e^{\Phi t}\Xi + e^{\Phi t}\left(g_3 h_v N(\zeta) + 1\right)\dot{\zeta} \tag{72}$$

$$\begin{aligned}V(t) \leq & \left(V(0) - \frac{\Xi}{\Phi}\right)e^{-\Phi t} + \frac{\Xi}{\Phi} \\ & + e^{-\Phi t}\int_0^t \left(g_3 h_v N(\zeta) + 1\right)\dot{\zeta} e^{\Phi\tau} d\tau\end{aligned} \tag{73}$$

Define $P_0 = \left(V(0) - \frac{\Xi}{\Phi}\right)e^{-\Phi t} + \frac{\Xi}{\Phi}$, based on Lemma 3 and [36], we can conclude that $\zeta, z_i (i = 1, 2, 3)$, and $\int_0^t \left(g_3 h(v) N(\zeta) + 1\right)\dot{\zeta} e^{\Phi\tau} d\tau$ are uniformly ultimately bounded.

Then according to (65), the following conditions are satisfied

$$|z_i| \leq \sqrt{2\left(P_0 + e^{-\Phi t}\int_0^t \left(g_3 h_v N(\zeta) + 1\right)\dot{\zeta} e^{\Phi\tau} d\tau\right)}, \quad i = 1, 2, 3 \tag{74}$$

Moreover, the tracking errors e_1, e_2, e_3 are also bounded because z_1, z_2, z_3 and ω_i are bounded. Then, the system states $x_i, i = 1, 2, 3$ are also bounded by the selection of design parameters. Thus, the proposed control can guarantee the dynamic behavior of the system under the influence of the unknown nonlinear dynamics and various loads of passengers.

Remark 7: To obtain the objectives of active suspension, the control parameters should be chosen to meet the balance between the demand of output performance and the actual operating conditions of the system. The PPF constraint is designed to satisfy the initial condition $-\underline{\kappa}\rho(t) < x_1 < \bar{\kappa}\rho(t)$ by selecting the boundary parameters $\underline{\kappa}, \bar{\kappa}, \rho_0$. A good control performance can be achieved with large φ and small ρ_∞ but lead to large control actions. Besides, the positive parameters R_1 and R_2 of Levant differentiators are designed to obtain the differential signals and guarantee the convergence of the filter in a finite-time. The large control gains k_i could enhance the convergence rate of the system but they require more control actions and lead to high chattering.

D. HANDLING STABILITY AND ROAD HOLDING ANALYSIS

In the previous analysis, the proposed control scheme has been designed to demonstrate the stability of the suspension system. By introducing a PPF constraint, the sprung mass displacement is guaranteed within the prescribed performance boundaries, which means the first objective of ride comfort is achieved. Other suspension requirements for handling stability and road holding are also analyzed in this section by choosing the appropriate control parameters.

Firstly, we consider the dynamic equations of the unsprung mass of the system (11). Based on the above results, the tracking errors $e_i, i = 1, 2, 3$ are proved to be bounded. Besides, the RBFNNs are used to approximate the unknown continuous function $f_2(X_2)$. Then, substituting (48) into (11), we obtain

$$\dot{X} = MX + NY + Y_0 \tag{75}$$

where

$$X = \begin{bmatrix} x_3 \\ x_4 \end{bmatrix}; \quad M = \begin{bmatrix} 0 & 1 \\ -\frac{k_t}{m_u} & -\frac{c_t}{m_u} \end{bmatrix}; \quad N = \begin{bmatrix} 0 & 0 \\ \frac{k_t}{m_u} & \frac{c_t}{m_u} \end{bmatrix};$$

$$Y = \begin{bmatrix} z_r \\ \dot{z}_r \end{bmatrix}$$

$$Y_0 = \begin{bmatrix} 0 \\ \Upsilon \end{bmatrix}; \Upsilon = \frac{m_s}{m_u}\left(W_2^T S_2(X_2) + \eta_2(X_2)\right) + \frac{m_s}{m_u}\left(-x_5 - d(t)\right)$$

Because the tracking errors e_i are bounded, Υ is also bounded and there is a constant $\bar{\Upsilon}$ such that $\|\Upsilon\| \leq \bar{\Upsilon}$.

Choose a Lyapunov function as follows

$$V_z = X^T P X \tag{76}$$

where P is a positive definite symmetric matrix.

Then, the time derivative of V_z is written as

$$\dot{V}_z = \dot{X}^T P X + X^T P \dot{X} \tag{77}$$

Substituting (75) into (77), we obtain

$$\dot{V}_z = X^T\left(M^T P + PM\right)X + 2X^T PNY + 2X^T P Y_0 \tag{78}$$

There is a positive definite symmetric matrix $Q > 0$ so that the Lyapunov equation $M^T P + PM = -Q$ is satisfied. Applying Young's inequality theorem, we can rewrite $2X^T PNY$ and $2X^T PY_0$ as follows

$$\begin{aligned} 2X^T PNY &\le \frac{1}{\gamma_1} X^T PNN^T PX + \gamma_1 Y^T Y \\ 2X^T PY_0 &\le \frac{1}{\gamma_2} X^T PPX + \gamma_2 Y_0^T Y_0 \end{aligned} \tag{79}$$

where $\gamma_1 > 0$ and $\gamma_2 > 0$ are the positive constants.

According to (79), we can write (78) as follows

$$\begin{aligned} \dot{V}_z \le & -\left\{ \begin{array}{l} \lambda_{\min}\left(P^{-1/2} Q P^{-1/2}\right) - \frac{1}{\gamma_1}\lambda_{\max}\left(P^{1/2} N N^T P^{1/2}\right) \\ \qquad - \frac{1}{\gamma_2}\lambda_{\max}(P) \end{array} \right\} V \\ & + \gamma_1 Y^T Y + \gamma_2 Y_0^T Y_0 \end{aligned} \tag{80}$$

where $\lambda_{\max}$ and $\lambda_{\min}$ denote the maximal and minimal eigenvalues of the matrix

Choose the positive constants γ_1, γ_2, and appropriate matrix P, Q, we obtain

$$\begin{aligned} \gamma_1 &> 2\frac{\lambda_{\max}\left(P^{1/2} N N^T P^{1/2}\right)}{\lambda_{\min}\left(P^{-1/2} Q P^{-1/2}\right)} \quad \text{and} \\ \gamma_2 &> 2\frac{\lambda_{\max}(P)}{\lambda_{\min}\left(P^{-1/2} Q P^{-1/2}\right)} \end{aligned} \tag{81}$$

From (81), there are two constants χ and ψ satisfying

$$\begin{aligned} \chi \ge & \lambda_{\min}\left(P^{-1/2} Q P^{-1/2}\right) - \frac{1}{\gamma_1}\lambda_{\max}\left(P^{1/2} N N^T P^{1/2}\right) \\ & - \frac{1}{\gamma_2}\lambda_{\max}(P) \end{aligned} \tag{82}$$

$$\psi \ge \gamma_1 Y^T Y + \gamma_2 Y_0^T Y_0 \tag{83}$$

Substituting (82) and (83) into (80), the time derivative of V_z is described by

$$\dot{V}_z \le -\chi V_z + \psi \tag{84}$$

Then, integrating both sides of equation (84), we obtain

$$V_z \le \left(V_z(0) - \frac{\psi}{\chi}\right) e^{-\chi t} + \frac{\psi}{\chi} \le V_z(0)\, e^{-\chi t} + \frac{\psi}{\chi} \tag{85}$$

Based on the above results, the system x_3 and x_4 are satisfied

$$|x_i(t)| \le \sqrt{\left(V_z(0)\, e^{-\chi t} + \frac{\psi}{\chi}\right)/\lambda_{\min}(P)}, \quad i = 3, 4 \tag{86}$$

From (15), the handling stability condition can be written as follows

$$\begin{aligned} |z_s - z_u| \le |x_1| + |x_3| \le \bar{\kappa}\rho(0) \\ + \sqrt{\left(V_z(0)\, e^{-\chi t} + \frac{\psi}{\chi}\right)/\lambda_{\min}(P)} \end{aligned} \tag{87}$$

Therefore, the inequality (15) is satisfied by selecting the PPF parameters $\bar{\kappa}, \underline{\kappa}, \rho(0)$ and the positive parameters γ_1, γ_2, P such that $|z_s - z_u| \le z_R$.

Similarly, the tire forces F_{st} and F_{dt} are computed by

$$\begin{aligned} F_{st}(z_u, z_r, t) &= k_t(x_3 - z_r) \\ &\le k_t\sqrt{\left(V_z(0)\, e^{-\chi t} + \frac{\psi}{\chi}\right)/\lambda_{\min}(P)} \\ &\quad + k_t \|z_r\|_\infty \end{aligned} \tag{88}$$

$$\begin{aligned} F_{dt}(z_u, z_r, t) &= c_t(x_4 - \dot{z}_r) \\ &\le c_t\sqrt{\left(V_z(0)\, e^{-\chi t} + \frac{\psi}{\chi}\right)/\lambda_{\min}(P)} \\ &\quad + c_t \|\dot{z}_r\|_\infty \end{aligned} \tag{89}$$

Substituting (88) and (89) into (2), we can get the relative tire force condition (16) as

$$\begin{aligned} |F_{st} + F_{dt}| &\le |F_{st} + F_{dt}| \\ &\le (k_t + c_t)\sqrt{\left(V_z(0)\, e^{-\chi t} + \frac{\psi}{\chi}\right)/\lambda_{\min}(P)} \\ &\quad + k_t\|z_r\|_\infty + c_t\|\dot{z}\|_\infty \end{aligned} \tag{90}$$

From (90), the RTF constraints can be obtained by selecting the positive parameters γ_1, γ_2, and matrix P to ensure $|F_{st} + F_{dt}| \le (m_s(t) + m_u)\, g$.

Based on the above analysis, the requirements of handling stability and road holding are satisfied by the selection of initial conditions and control parameters.

Remark 8: The proposed control can ensure not only the transient response of vertical displacement of the sprung mass but also the mechanical structure and safety condition of the pneumatic suspension. Furthermore, by choosing the appropriate PPF constraints and control design parameters, the proposed control can improve the performance requirements of pneumatic active suspension.

IV. SIMULATION RESULTS AND DISCUSSION

A. SIMULATION DESCRIPTION

In this section, the numerical simulation examples for pneumatic active suspension are provided to demonstrate the effectiveness of the proposed method compared with passive suspension, traditional backstepping, CFC, and PPF controllers. To evaluate the ride comfort of active suspension, in addition to reducing the sprung mass displacement, the human body's sensitivity to acceleration should be considered during the control design process. According to ISO 2361 criteria, humans are sensitive to vertical vibration in the frequency range of 4 - 8 Hz, and the active suspension systems must be guaranteed to a minimum in this domain. Therefore, the root mean square (RMS) values of sprung mass acceleration are examined with a filter is proposed in [58].

$$W(s) = \frac{81.89s^3 + 796.6s^2 + 1937s + 0.1446}{s^4 + 80s^3 + 2264s^2 + 7172s + 21196} \tag{91}$$

Besides, the objectives of handling stability and road holding are also investigated in this study by considering

two parameters RSD and RTF. The main parameters of pneumatic active suspension are listed in Table 2.

TABLE 2. Pneumatic active suspension parameters.

Parameter	Value	Unit
m_s	$550 \pm 100\sin(\pi t)$	kg
m_u	60	kg
k_s	16000	Nm^{-1}
k_t	145000	Nm^{-1}
c_a	2300	Nsm^{-1}
c_t	1100	Nsm^{-1}
z_R	0.04	m
z_{as0}	0.18	m
R	287.5	$J.Kg^{-1}.K^{-1}$
A_{as}	0.0047	m^2
γ	1.4	-
T	293.15	K

The simulation examples are demonstrated by the sin road profile with amplitude 0.02 m and frequency 1 Hz as $z_r = 0.02\sin(2\pi t)$. The initial values of the system states are set by $x_1(0) = 0.05\ (m)$, $x_2(0) = x_3(0) = x_4(0) = 0\ (m)$, $x_5(0) = 0.5 \times 10^5\ (Pa)$. The PPF constraint is defined by $\rho_0 = 0.058$, $\rho_\infty = 0.0029$, $\varphi = 1.5$ and design parameters $\kappa = 0.98$, $\bar{\kappa} = 0.98$. To investigate the comparative results, the control parameters are given in Table 3.

TABLE 3. Control parameters.

Control	Parameters
Backstepping	$k_1 = 35; k_2 = 25; k_3 = 10$
CFC	$k_1 = 35; k_2 = 25; k_3 = 10$
	$R_1 = 40; R_2 = 100; r_2 = 0.1; r_3 = 0.1$
PPF	$k_1 = 35; k_2 = 25; k_3 = 10$
	$\rho_0 = 0.058, \rho_\infty = 0.0029, \varphi = 1.5$
Proposed	$k_1 = 35; k_2 = 25; k_3 = 10$
	$R_1 = 40; R_2 = 100; r_2 = 0.1; r_3 = 0.1$
	$m = 1; q = 1; n = 20; \xi = 0.01;$

B. SIMULATION RESULTS

The comparative simulation results of sprung mass acceleration and displacement, relative suspension deflection, relative tire force, and control signals of passive, traditional backstepping, CFC, PPF, and proposed control with sin road profile are provided in Figs. 3–7. The passenger comfort, driving safety, and handling stability are strongly improved

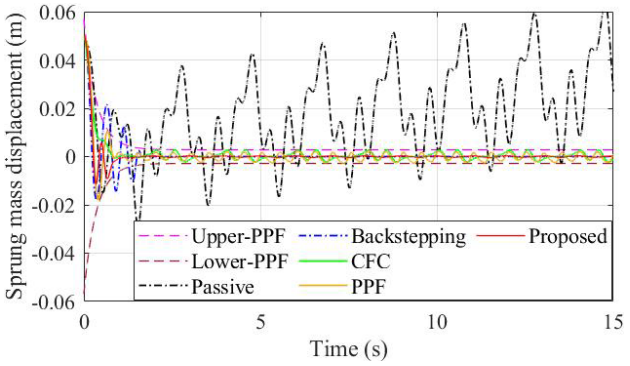

FIGURE 3. Comparative performance of sprung mass displacements.

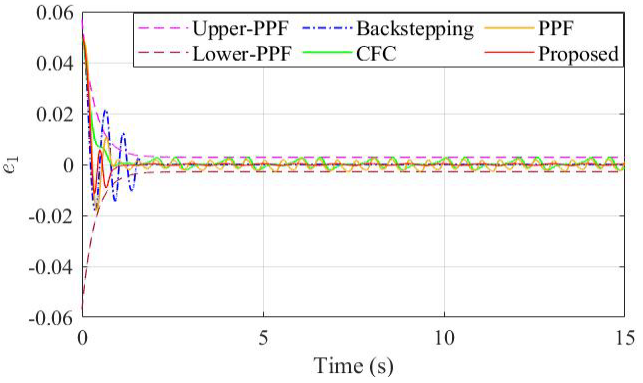

FIGURE 4. Vertical displacement tracking errors of sprung mass.

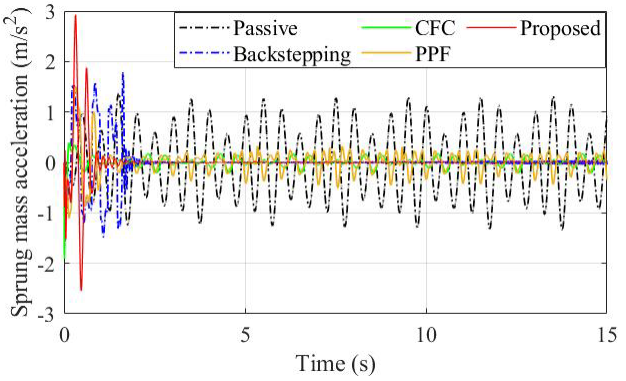

FIGURE 5. Acceleration responses of the sprung mass.

with the proposed control because the responses of acceleration and deflection, RSD, and RTF are all guaranteed. The proposed control can enhance the ride comfort compared with the other methods because the sprung mass displacement is ensured inside the boundary constraints as shown in Fig. 3. In particular, the proposed control can obtain better regulation performance and ensure the convergence of the tracking error does not violate the maximum overshoot as shown in Fig. 4. By introducing the PPF constraint, the time of zero convergence for the error signal e_1 can be achieved faster and around $t = 1.3\ (s)$. Although CFC can reduce the sprung mass displacement compared with passive suspension, there

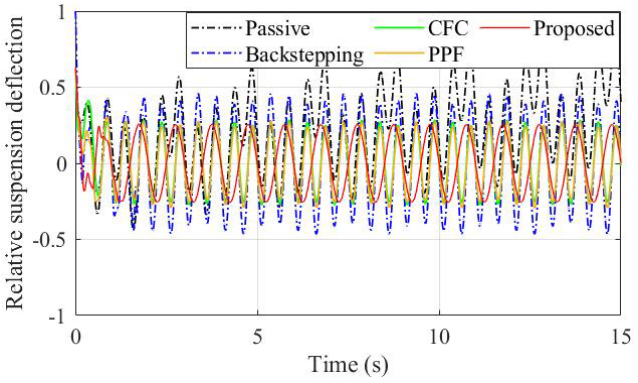

FIGURE 6. Relative suspension deflection responses.

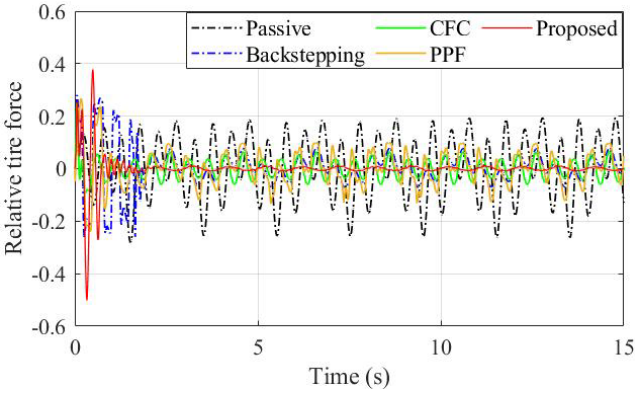

FIGURE 7. Relative tire force responses.

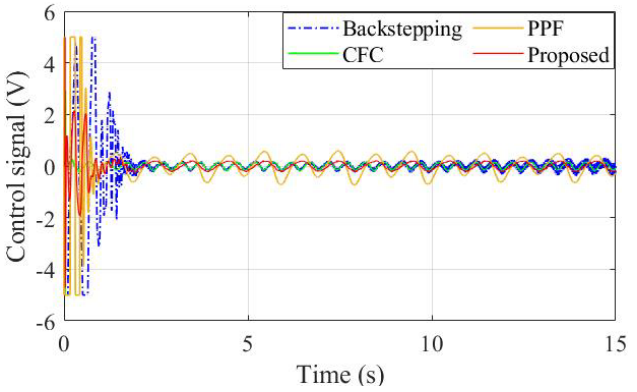

FIGURE 8. Control signals (V).

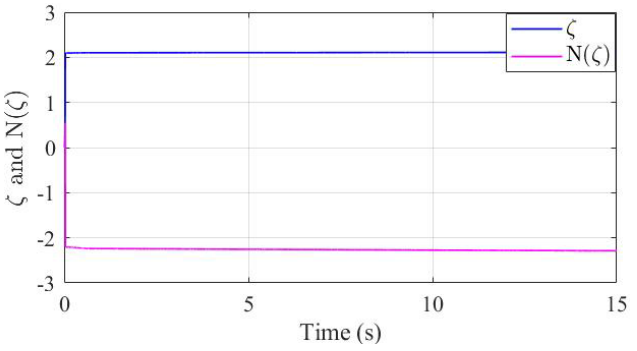

FIGURE 9. Simulation results of Nussbaum gain.

are some peak values due to external disturbance that can affect the passenger comfort. Besides, the PPF control can guarantee the tracking error of vertical displacement within the boundaries but it cannot converge to zero because of parametric uncertainties. As can be seen in Fig. 4, the traditional backstepping cannot fulfill the convergence time requirement of the prescribed performance constraint. In addition, the proposed control can provide the magnitude of the RSD smaller than other methods as shown in Fig. 6, and this RSD is also guaranteed to be less than 1. Due to the influence of uncertain parameters in the dynamic system, the RSD of passive suspension is the biggest value, and there are some maximum peak points. Furthermore, the traditional backstepping cannot provide a good performance of RSD because it is affected by unknown parameters. By keeping the sprung mass vibration under the PPF boundaries, the proposed control scheme can not only provide passenger comfort but also guarantee the magnitude of RSD and RTF within the limit values. From Fig. 7, the dynamic stroke constraints are guaranteed within the limits to ensure the stability of the chassis. Moreover, the RTF value of the proposed control is also smaller than CFC, PPF, and traditional backstepping designs.

The comparative simulation results of control signals are shown in Fig. 8. The objectives of suspension can be guaranteed in the presence of pneumatic actuator saturation with the proposed control. The control signals of PPF and traditional backstepping controllers are larger and more chattering than the proposed control because of external disturbances. The CFC scheme can avoid the chattering problem of traditional backstepping control. Compared with the basic control designs, the proposed control scheme with NNs can overcome the unknown parameters to provide good performance for pneumatic active suspension. Besides, the simulation results of Nussbaum function signals ζ and $N(\zeta)$ are shown in Fig. 9. It can be seen clearly that the Nussbaum gain $N(\zeta)$ moves in to correct direction to ensure the tracking performance.

V. CONCLUSION

This paper presents an adaptive neural command filtered control with prescribed performance and input saturation for the pneumatic active suspension system. The proposed control scheme can not only retain sprung mass vertical displacement within the prescribed performance boundaries to get the ride comfort but also guarantee handling stability and road holding. To approximate the unknown continuous functions of the pneumatic suspension system with an air spring actuator, the RBFNNs are developed in the control design. In addition, the Gaussian error function is employed to characterize the saturation nonlinearity as a continuous differentiable form, and the Nussbaum gain function is then applied to scope with unknown control directions of pneumatic active suspension. A command filtered backstepping control has been employed to solve the explosion of complexity in traditional backstepping designs. Finally, the effectiveness of the

proposed control is verified by the simulation examples which indicate that the controller design can be more efficient than other adaptive controllers. Therefore, this approach can be a promising method for the automotive industry.

REFERENCES

[1] M. W. Holtz and J. L. van Niekerk, "Modelling and design of a novel air-spring for a suspension seat," *J. Sound Vibrat.*, vol. 329, no. 21, pp. 4354–4366, Oct. 2010, doi: 10.1016/j.jsv.2010.04.017.

[2] H. Kim and H. Lee, "Height and leveling control of automotive air suspension system using sliding mode approach," *IEEE Trans. Veh. Technol.*, vol. 60, no. 5, pp. 2027–2041, Jun. 2011, doi: 10.1109/tvt.2011.2138730.

[3] H. Du and N. Zhang, "Fuzzy control for nonlinear uncertain electrohydraulic active suspensions with input constraint," *IEEE Trans. Fuzzy Syst.*, vol. 17, no. 2, pp. 343–356, Apr. 2009, doi: 10.1109/tfuzz.2008.2011814.

[4] T. P. J. van der Sande, B. L. J. Gysen, I. J. M. Besselink, J. J. H. Paulides, E. A. Lomonova, and H. Nijmeijer, "Robust control of an electromagnetic active suspension system: Simulations and measurements," *Mechatronics*, vol. 23, no. 2, pp. 204–212, Mar. 2013, doi: 10.1016/j.mechatronics.2012.07.002.

[5] G. S. Prassad and M. K. Mohan, "A contemporary adaptive air suspension using LQR control for passenger vehicles," *ISA Trans.*, vol. 93, pp. 244–254, Oct. 2019, doi: 10.1016/j.isatra.2019.02.031.

[6] X. Ma, P. K. Wong, J. Zhao, J.-H. Zhong, H. Ying, and X. Xu, "Design and testing of a nonlinear model predictive controller for ride height control of automotive semi-active air suspension systems," *IEEE Access*, vol. 6, pp. 63777–63793, 2018, doi: 10.1109/ACCESS.2018.2876496.

[7] L. He, W. Xu, W. Bu, and L. Shi, "Dynamic analysis and design of air spring mounting system for marine propulsion system," *J. Sound Vibrat.*, vol. 333, no. 20, pp. 4912–4929, Sep. 2014, doi: 10.1016/j.jsv.2014.05.045.

[8] J.-J. Chen, Z.-H. Yin, S. Rakheja, J.-H. He, and K.-H. Guo, "Theoretical modelling and experimental analysis of the vertical stiffness of a convoluted air spring including the effect of the stiffness of the bellows," *Proc. Inst. Mech. Eng., D, J. Automobile Eng.*, vol. 232, no. 4, pp. 547–561, Mar. 2018, doi: 10.1177/0954407017704589.

[9] R. Zhao, W. Xie, P. K. Wong, D. Cabecinhas, and C. Silvestre, "Robust ride height control for active air suspension systems with multiple unmodeled dynamics and parametric uncertainties," *IEEE Access*, vol. 7, pp. 59185–59199, 2019, doi: 10.1109/ACCESS.2019.2913451.

[10] A. J. Nieto, A. L. Morales, J. R. Trapero, J. M. Chicharro, and P. Pintado, "An adaptive pneumatic suspension based on the estimation of the excitation frequency," *J. Sound Vibrat.*, vol. 330, no. 9, pp. 1891–1903, Apr. 2011, doi: 10.1016/j.jsv.2010.11.009.

[11] P. Karimi Eskandary, A. Khajepour, A. Wong, and M. Ansari, "Analysis and optimization of air suspension system with independent height and stiffness tuning," *Int. J. Automot. Technol.*, vol. 17, no. 5, pp. 807–816, Oct. 2016, doi: 10.1007/s12239-016-0079-9.

[12] J. Xiao, B. T. Kulakowski, and M. Cao, "Active air-suspension design for transit buses," *Int. J. Heavy Vehicle Syst.*, vol. 14, no. 4, pp. 421–440, 2007.

[13] X. Sun, C. Yuan, Y. Cai, S. Wang, and L. Chen, "Model predictive control of an air suspension system with damping multi-mode switching damper based on hybrid model," *Mech. Syst. Signal Process.*, vol. 94, pp. 94–110, Sep. 2017, doi: 10.1016/j.ymssp.2017.02.033.

[14] X. Sun, Y. Cai, L. Chen, Y. Liu, and S. Wang, "Vehicle height and posture control of the electronic air suspension system using the hybrid system approach," *Vehicle Syst. Dyn.*, vol. 54, no. 3, pp. 328–352, Mar. 2016, doi: 10.1080/00423114.2015.1136425.

[15] J. Yu, P. Shi, and L. Zhao, "Finite-time command filtered backstepping control for a class of nonlinear systems," *Automatica*, vol. 92, pp. 173–180, Jun. 2018, doi: 10.1016/j.automatica.2018.03.033.

[16] J. Ma, Z. Zheng, and P. Li, "Adaptive dynamic surface control of a class of nonlinear systems with unknown direction control gains and input saturation," *IEEE Trans. Cybern.*, vol. 45, no. 4, pp. 728–741, Apr. 2015, doi: 10.1109/TCYB.2014.2334695.

[17] D. Swaroop, J. K. Hedrick, P. P. Yip, and J. C. Gerdes, "Dynamic surface control for a class of nonlinear systems," *IEEE Trans. Autom. Control*, vol. 45, no. 10, pp. 1893–1899, Oct. 2000.

[18] S.-C. Tong, Y.-M. Li, G. Feng, and T.-S. Li, "Observer-based adaptive fuzzy backstepping dynamic surface control for a class of MIMO nonlinear systems," *IEEE Trans. Syst., Man, Cybern. B, Cybern.*, vol. 41, no. 4, pp. 1124–1135, Aug. 2011, doi: 10.1109/TSMCB.2011.2108283.

[19] J. Na, J. Yang, S. Wang, G. Gao, and C. Yang, "Unknown dynamics estimator-based output-feedback control for nonlinear pure-feedback systems," *IEEE Trans. Syst., Man, Cybern. Syst.*, early access, Aug. 20, 2019, doi: 10.1109/tsmc.2019.2931627.

[20] J. A. Farrell, M. Polycarpou, M. Sharma, and W. Dong, "Command filtered backstepping," *IEEE Trans. Autom. Control*, vol. 54, no. 6, pp. 1391–1395, Jun. 2009, doi: 10.1109/tac.2009.2015562.

[21] W. Dong, J. A. Farrell, M. M. Polycarpou, V. Djapic, and M. Sharma, "Command filtered adaptive backstepping," *IEEE Trans. Control Syst. Technol.*, vol. 20, no. 3, pp. 566–580, May 2012, doi: 10.1109/tcst.2011.2121907.

[22] J. Yu, P. Shi, W. Dong, and C. Lin, "Adaptive fuzzy control of nonlinear systems with unknown dead zones based on command filtering," *IEEE Trans. Fuzzy Syst.*, vol. 26, no. 1, pp. 46–55, Feb. 2018, doi: 10.1109/tfuzz.2016.2634162.

[23] Q. Chen, Y. Ye, Z. Hu, J. Na, and S. Wang, "Finite-time approximation-free attitude control of quadrotors: Theory and experiments," *IEEE Trans. Aerosp. Electron. Syst.*, early access, Jan. 19, 2021. [Online]. Available: https://ieeexplore.ieee.org/document/9328470

[24] J. Qiu, K. Sun, I. J. Rudas, and H. Gao, "Command filter-based adaptive NN control for MIMO nonlinear systems with full-state constraints and actuator hysteresis," *IEEE Trans. Cybern.*, vol. 50, no. 7, pp. 2905–2915, Jul. 2020, doi: 10.1109/TCYB.2019.2944761.

[25] S. Li, C. K. Ahn, and Z. Xiang, "Command-filter-based adaptive fuzzy finite-time control for switched nonlinear systems using state-dependent switching method," *IEEE Trans. Fuzzy Syst.*, vol. 29, no. 4, pp. 833–845, Apr. 2021, doi: 10.1109/tfuzz.2020.2965917.

[26] R. M. Sanner and J.-J.-E. Slotine, "Gaussian networks for direct adaptive control," *IEEE Trans. Neural Netw.*, vol. 3, no. 6, pp. 837–863, Nov. 1992.

[27] K. K. Ahn and H. P. H. Anh, "Comparative study of modeling and identification of the pneumatic artificial muscle (PAM) manipulator using recurrent neural networks," *J. Mech. Sci. Technol.*, vol. 22, no. 7, pp. 1287–1298, Jul. 2008, doi: 10.1007/s12206-008-0416-7.

[28] D. X. Ba, T. Q. Dinh, and K. K. Ahn, "An integrated intelligent nonlinear control method for a pneumatic artificial muscle," *IEEE/ASME Trans. Mechatronics*, vol. 21, no. 4, pp. 1835–1845, Aug. 2016, doi: 10.1109/TMECH.2016.2558292.

[29] J. Zhao, P. King Wong, Z. Xie, C. Wei, and F. He, "Integrated variable speed-fuzzy PWM control for ride height adjustment of active air suspension systems," in *Proc. Amer. Control Conf. (ACC)*, Jul. 2015, pp. 5700–5705.

[30] W.-N. Bao, L.-P. Chen, Y.-Q. Zhang, and Y.-S. Zhao, "Fuzzy adaptive sliding mode controller for an air spring active suspension," *Int. J. Automot. Technol.*, vol. 13, no. 7, pp. 1057–1065, Dec. 2012, doi: 10.1007/s12239-012-0108-2.

[31] J. Na, Q. Chen, X. Ren, and Y. Guo, "Adaptive prescribed performance motion control of servo mechanisms with friction compensation," *IEEE Trans. Ind. Electron.*, vol. 61, no. 1, pp. 486–494, Jan. 2014, doi: 10.1109/tie.2013.2240635.

[32] K. K. Ahn and H. P. H. Anh, "Design and implementation of an adaptive recurrent neural networks (ARNN) controller of the pneumatic artificial muscle (PAM) manipulator," *Mechatronics*, vol. 19, no. 6, pp. 816–828, Sep. 2009, doi: 10.1016/j.mechatronics.2009.04.006.

[33] U. S. Pusadkar, S. D. Chaudhari, P. D. Shendge, and S. B. Phadke, "Linear disturbance observer based sliding mode control for active suspension systems with non-ideal actuator," *J. Sound Vibrat.*, vol. 442, pp. 428–444, Mar. 2019, doi: 10.1016/j.jsv.2018.11.003.

[34] J. Ma, S. S. Ge, Z. Zheng, and D. Hu, "Adaptive NN control of a class of nonlinear systems with asymmetric saturation actuators," *IEEE Trans. Neural Netw. Learn. Syst.*, vol. 26, no. 7, pp. 1532–1538, Jul. 2015, doi: 10.1109/TNNLS.2014.2344019.

[35] S. S. Ge and C. Wang, "Direct adaptive NN control of a class of nonlinear systems," *IEEE Trans. Neural Netw.*, vol. 13, no. 1, pp. 214–221, Aug. 2002.

[36] S. Sam Ge and J. Wang, "Robust adaptive tracking for time-varying uncertain nonlinear systems with unknown control coefficients," *IEEE Trans. Autom. Control*, vol. 48, no. 8, pp. 1463–1469, Aug. 2003, doi: 10.1109/tac.2003.815049.

[37] S. S. Ge, F. Hong, and T. H. Lee, "Adaptive neural control of nonlinear time-delay systems with unknown virtual control coefficients," *IEEE Trans. Syst., Man Cybern. B, Cybern.*, vol. 34, no. 1, pp. 499–516, Feb. 2004, doi: 10.1109/tsmcb.2003.817055.

[38] W. Wang, D. Wang, Z. Peng, and T. Li, "Prescribed performance consensus of uncertain nonlinear strict-feedback systems with unknown control directions," *IEEE Trans. Syst., Man, Cybern. Syst.*, vol. 46, no. 9, pp. 1279–1286, Sep. 2016, doi: 10.1109/tsmc.2015.2486751.
[39] F. Shojaei, M. M. Arefi, A. Khayatian, and H. R. Karimi, "Observer-based fuzzy adaptive dynamic surface control of uncertain nonstrict feedback systems with unknown control direction and unknown dead-zone," *IEEE Trans. Syst., Man, Cybern. Syst.*, vol. 49, no. 11, pp. 2340–2351, Nov. 2019, doi: 10.1109/tsmc.2018.2852725.
[40] C. P. Bechlioulis and G. A. Rovithakis, "Robust adaptive control of feedback linearizable MIMO nonlinear systems with prescribed performance," *IEEE Trans. Autom. Control*, vol. 53, no. 9, pp. 2090–2099, Oct. 2008, doi: 10.1109/tac.2008.929402.
[41] Y.-J. Liu and H. Chen, "Adaptive sliding mode control for uncertain active suspension systems with prescribed performance," *IEEE Trans. Syst., Man, Cybern. Syst.*, early access, Jan. 13, 2020, doi: 10.1109/tsmc.2019.2961927.
[42] S. Wang, J. Na, and Q. Chen, "Adaptive predefined performance sliding mode control of motor driving systems with disturbances," *IEEE Trans. Energy Convers.*, early access, Nov. 16, 2020, doi: 10.1109/tec.2020.3038010.
[43] C. Zhang, J. Na, J. Wu, Q. Chen, and Y. Huang, "Proportional-integral approximation-free control of robotic systems with unknown dynamics," *IEEE/ASME Trans. Mechatronics*, early access, Nov. 3, 2020, doi: 10.1109/tmech.2020.3035660.
[44] J. Na, Y. Huang, X. Wu, G. Gao, G. Herrmann, and J. Z. Jiang, "Active adaptive estimation and control for vehicle suspensions with prescribed performance," *IEEE Trans. Control Syst. Technol.*, vol. 26, no. 6, pp. 2063–2077, Nov. 2018, doi: 10.1109/TCST.2017.2746060.
[45] Y.-J. Liu, Q. Zeng, S. Tong, C. L. P. Chen, and L. Liu, "Actuator failure compensation-based adaptive control of active suspension systems with prescribed performance," *IEEE Trans. Ind. Electron.*, vol. 67, no. 8, pp. 7044–7053, Aug. 2020, doi: 10.1109/tie.2019.2937037.
[46] A. K. Kostarigka and G. A. Rovithakis, "Adaptive dynamic output feedback neural network control of uncertain MIMO nonlinear systems with prescribed performance," *IEEE Trans. Neural Netw. Learn. Syst.*, vol. 23, no. 1, pp. 138–149, Jan. 2012, doi: 10.1109/TNNLS.2011.2178448.
[47] H. Liu, X. Li, X. Liu, and H. Wang, "Adaptive neural network prescribed performance bounded- H_∞ tracking control for a class of stochastic nonlinear systems," *IEEE Trans. Neural Netw. Learn. Syst.*, vol. 31, no. 6, pp. 2140–2152, Jun. 2020, doi: 10.1109/TNNLS.2019.2928594.
[48] W. Shi, R. Luo, and B. Li, "Adaptive fuzzy prescribed performance control for MIMO nonlinear systems with unknown control direction and unknown dead-zone inputs," *ISA Trans.*, vol. 66, pp. 86–95, Jan. 2017, doi: 10.1016/j.isatra.2016.08.021.
[49] D. Zhai, C. Xi, L. An, J. Dong, and Q. Zhang, "Prescribed performance switched adaptive dynamic surface control of switched nonlinear systems with average dwell time," *IEEE Trans. Syst., Man, Cybern. Syst.*, vol. 47, no. 7, pp. 1257–1269, Jul. 2017, doi: 10.1109/tsmc.2016.2571338.
[50] C. Kim and P. I. Ro, "A sliding mode controller for vehicle active suspension systems with non-linearities," *Proc. Inst. Mech. Eng., D, J. Automobile Eng.*, vol. 212, no. 2, pp. 79–92, Feb. 1998.
[51] F. de Melo, A. Pereira, and A. Morais, "The simulation of an automotive air spring suspension using a pseudo-dynamic procedure," *Appl. Sci.*, vol. 8, no. 7, pp. 1049–1068, 2018, doi: 10.3390/app8071049.
[52] C. Wen, J. Zhou, Z. Liu, and H. Su, "Robust adaptive control of uncertain nonlinear systems in the presence of input saturation and external disturbance," *IEEE Trans. Autom. Control*, vol. 56, no. 7, pp. 1672–1678, Jul. 2011, doi: 10.1109/tac.2011.2122730.
[53] Y.-J. Liu, J. Li, S. Tong, and C. L. P. Chen, "Neural network control-based adaptive learning design for nonlinear systems with full-state constraints," *IEEE Trans. Neural Netw. Learn. Syst.*, vol. 27, no. 7, pp. 1562–1571, Jul. 2016, doi: 10.1109/TNNLS.2015.2508926.
[54] Y. Xudong and J. Jingping, "Adaptive nonlinear design without a priori knowledge of control directions," *IEEE Trans. Autom. Control*, vol. 43, no. 11, pp. 1617–1621, Nov. 1998.
[55] A. Levant, "Higher-order sliding modes, differentiation and output-feedback control," *Int. J. Control*, vol. 76, nos. 9–10, pp. 924–941, Jan. 2003, doi: 10.1080/0020717031000099029.
[56] A. Levant, "Robust exact differentiation via sliding mode technique," *Automatica*, vol. 34, no. 3, pp. 379–384, Mar. 1998.
[57] Y. Huang, J. Na, X. Wu, X. Liu, and Y. Guo, "Adaptive control of nonlinear uncertain active suspension systems with prescribed performance," *ISA Trans.*, vol. 54, pp. 145–155, Jan. 2015, doi: 10.1016/j.isatra.2014.05.025.
[58] L. Zuo and S. A. Nayfeh, "Low order continuous-time filters for approximation of the ISO 2631-1 human vibration sensitivity weightings," *J. Sound Vibrat.*, vol. 265, no. 2, pp. 459–465, 2003, doi: 10.1016/s0022-460x(02)01567-5.

CONG MINH HO received the B.S. degree from the Department of Mechanical Engineering, Ho Chi Minh City University of Technology, Ho Chi Minh City, Vietnam, in 2008, and the M.S. degree from the Department of Mechanical Engineering, Ho Chi Minh City University of Technology and Education, in 2018. He is currently pursuing the Ph.D. degree with the School of Mechanical Engineering, University of Ulsan, Ulsan, South Korea.

His research interests include adaptive control, fluid power control, and active suspension systems.

DUC THIEN TRAN received the B.S. and M.S. degrees from the Department of Electrical Engineering, Ho Chi Minh City University of Technology, Vietnam, in 2010 and 2013, respectively, and the Ph.D. degree from the University of Ulsan, in 2020.

He currently works as a Lecturer with the Department of Automatic Control, Ho Chi Minh City University of Technology and Education (HCMUTE), Vietnam. His research interests include robotics, variable stiffness systems, fluid power control, disturbance observer, nonlinear control, adaptive control, and intelligent technique.

CONG HUNG NGUYEN was born in 1992. He received the B.S. degree from the Department of Mechanical Engineering, Ho Chi Minh City University of Technology, Ho Chi Minh City, Vietnam, in 2017. He is currently pursuing the M.Sc. degree with the School of Mechanical Engineering, University of Ulsan, Ulsan, South Korea.

His research interest includes vibration isolation.

KYOUNG KWAN AHN (Senior Member, IEEE) received the B.S. degree from the Department of Mechanical Engineering, Seoul National University, in 1990, the M.Sc. degree in mechanical engineering from the Korea Advanced Institute of Science and Technology, in 1992, and the Ph.D. degree from the Tokyo Institute of Technology, in 1999.

He is currently a Professor with the School of Mechanical Engineering, University of Ulsan, Ulsan, South Korea. His research interests include design and control of smart actuator using the smart material, fluid power control and active damping control, and renewable energy. He is also an Editor of *IJCAS* and an Editorial Board Member of *Renewable Energy*, *Actuators*, and *Journal of Engineering*.